94422

Report LR-705

The Numerical Simulation of the Collapse Process of Axially Compressed Cylindrical Shells with Measured Imperfections

E. Riks / C.C. Rankin / F.A. Brogan

TU Delft

Faculty of Aerospace Engineering

The Numerical Simulation of the Collapse Process of Axially Compressed Cylindrical Shells with Measured Imperfections

by

E. Riks , C.C. Rankin & F.A. Brogan

1. Introduction

Thin cylindrical shells in compression buckle explosively as is known from numerous experiments. What happens visually during the buckling phase has been revealed only at some isolated instances where high speed video recordings were made of these phenomena, see for example (Ref. 1). But as far as it is known the actual buckling process of a cylindrical shell has never been numerically simulated. We believe that the most likely reason for this is that the whole arsenal of computational tools that are necessary for this task were not yet available at the time such calculations were contemplated.

But the situation indicated above has changed. The potential of the present day finite element software and the power of the computer hardware has increased so much that the restrictions mentioned no longer exist. To illustrate this point we present here the numerical computation of the collapse process of a cylindrical shell under prescribed edge displacements. The shell that we chose for our computational experiment was manufactured, measured and tested some twenty years ago by Singer, Arbocz and Babcock under carefully controlled conditions in a laboratory environment (Ref. 2).

2. Description of the problem

In buckling experiments on cylindrical shells one chooses usually between two options of load application. The first is the case of dead weight loading by which the load is controlled in a direct way (Figure 1). In the second case, the load is introduced by means of a forced end-shortening controlled by the testing machine (Figure 2). For an introduction to the terminology and concepts that are used here refer to (Ref. 3).

If one wants the shell not to be destroyed in the testing machine, the second option of loading is to be preferred. In that case (Figure 2), the shell becomes unstable in a limit point for the end-shortening, rather than at a limit point for the load as in Figure 1. The dynamic snap that takes place in that case will be along the dotted vertical line in the figure, at least, in the ideal case that the end-shortening control is perfect. The snapping motion ends at a stable post-buckling state at value of the total load much smaller than the limit load. It is worth noting, that if the shell is fully clamped, the static pre-collapse equilibrium curves in both loading cases are identical because they are defined by sets of equations that are equivalent.

This is the reason that the *limit point* for the *load* in case 2 can be equated to the *limit point* for the *load* in case 1.

It is now possible to state the objective of our computational experiment. The objective is to compute the loading path I in figure 2 and the subsequent snap to the post-buckling state II. Of considerable interest is here the change in shape of the post-buckling displacement pattern during this process and the final shape that belongs to the post-buckled state II.

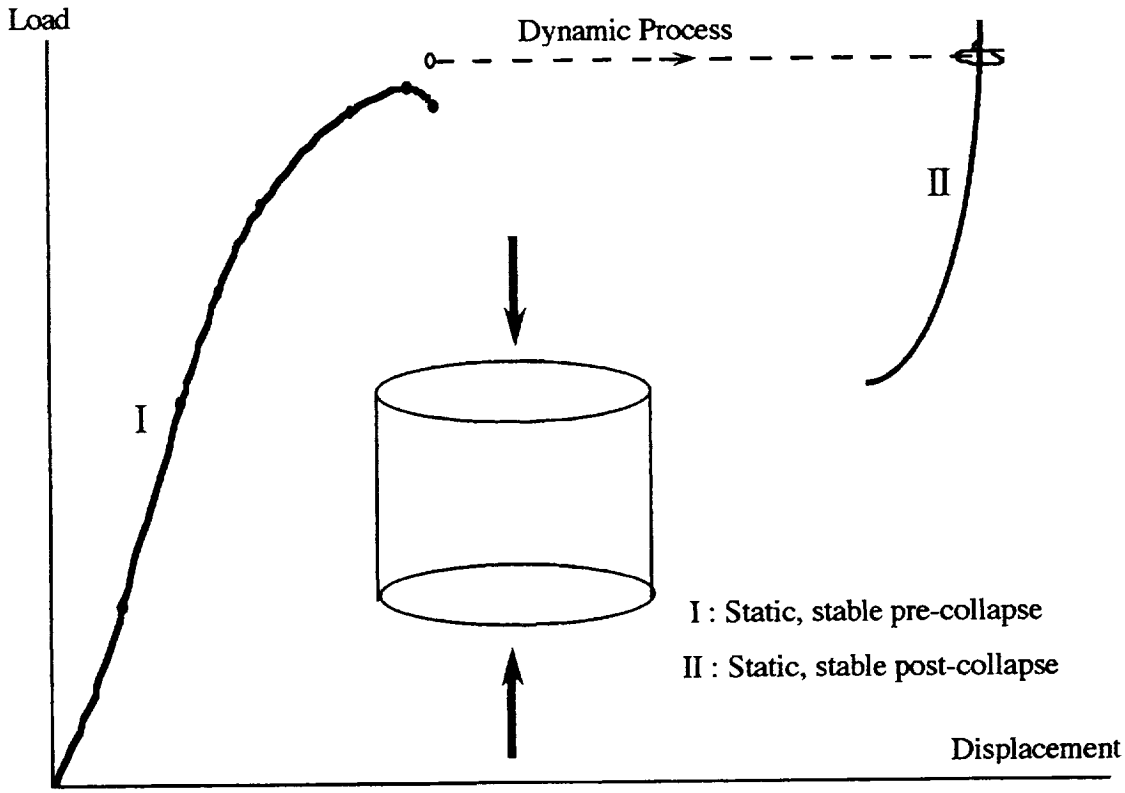

Figure 1 Simulation of a collapse process (dead weight loading)

3. Shell model used in the computations.

A detailed description of the test program dealing with the buckling tests is given in the reference already mentioned (Ref. 2). The test specimen, called AS2, is an integrally machined stringer stiffened cylindrical shell of which the deviations from the cylindrical form were carefully measured. During the experiment, the wave pattern in the pre-collapse state was observed to be dominated by a mode of one half wave in the axial direction and 9 waves in the circumferential direction. In the post-buckling state after the snap, the pattern had changed to one half wave in the axial direction and 10 full waves in the circumferential direction.

In (Ref. 4) computational models were defined for this shell with a geometry based on the measured imperfections. The models were used to check theory with experiment, that is

whether the collapse loads predicted by numerical models are anywhere near the experimentally determined collapse loads[1]. Because the computer facilities of the time were limited in capacity, the models were somewhat simplified in order to economize on the number of computational degrees of freedom that were needed. The simplifications basically concern the adaptation of some symmetry in the imperfection pattern and ensuing deformation after the load is applied.

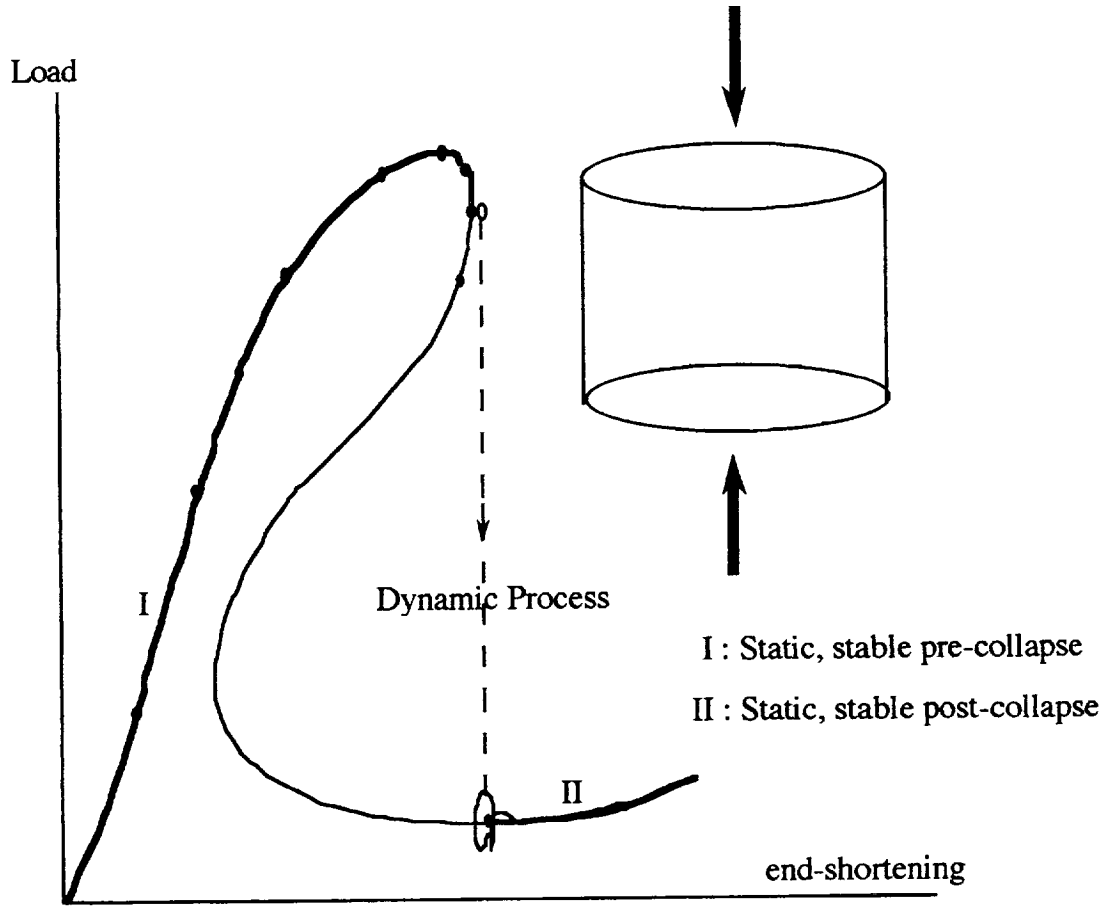

Figure 2 Simulation of a collapse process (prescribed end-shortening)

In this report, we will make use of one of these simplifications. It is the so-called 7 mode imperfection model which has two planes of symmetry. This is the mid-plane perpendicular to the axis and a plane through the axis. We chose this model not only to verify whether the results reported in (Ref. 4) could be reproduced but also because we did not want to start our computational experiment with the most demanding model in existence (in terms of degrees of freedom). It is true that the displacement pattern this model will take before collapse cannot

[1] They were.

be in agreement with the actual test result because the imperfection pattern simply lacks the appropriate terms. On the other hand it can be expected that the deep post-buckling state is not strongly influenced by the initial imperfections so that the post-buckling states of the model might show the general shape that was observed in the experiment (Ref. 4).

The calculations that we present here are carried out with the Q-STAGS shell finite element program , a modernized version of STAGS- C [STAGS = Structural Analysis of General Shells] (Ref. 5). In this program, the imperfections are introduced at the level of the strain measures. This means that the Green - Lagrange strains for the imperfect shell are computed as:

$$\gamma^*_{ij} = \frac{1}{2}(g_{ij} - g^0_{ij}) = \gamma_{ij}(\mathbf{u}) + \frac{1}{2}[(\mathbf{u}_{,i})^T \mathbf{u}^0_{,j} + (\mathbf{u}^0_{,i})^T \mathbf{u}_{,j}] \qquad (1)$$

where $(.)_{,i}$ = the usual notation for partial differentiation with respect to the reference coordinates, $\mathbf{u}^0$ are the deviations from the perfect cylindrical shape and $\mathbf{u}$ the displacements due to the deformation of the shell measured from the imperfect shape. The symbol γ_{ij} stands for the strain expressions calculated for the perfect shell. The imperfections are thus not simply introduced by displacing the nodes from the cylindrical surface, but they are calculated as extra contributions to the original strain measures for the perfect cylinder as it is done in the classical analytical imperfection sensitivity studies. Incidentally, the possibility to introduce imperfections in terms of a double Fourier expansion is a standard option in STAGS and we made gratefully use of it here.

For the computations it is only necessary to take into account one quarter of the shell with the given imperfection mode. However, for the sake of a more comprehensive visualization of the deformed shell, we took here into account a full length model of the shell segment of 180 degrees in circumferential direction. We used the standard shell element denoted by 410 (Ref. 6) to discretize the shell. This places the current analysis in the context of small strain - large rotation theory (Ref. 7, 8). The mesh that we selected was identical to that of (Ref. 4), i.e. $(2 \times 21) \times 131$ node points in axial and circumferential direction respectively, leading to approximately 25000 computational degrees of freedom. The boundary conditions at the loaded edges correspond to fully clamped.

4. Computations and results

The pre-collapse loading path was calculated with the standard path following method that is available in Q-STAGS (Refs. 9, 10). The typical shape of the pre-buckling state is pictured in Figure 3. When the limit point was passed, we took the solution $\mathbf{d}_k$ (which is unstable) closest to the limit point and used this value to formulate the initial conditions for a transient analysis but this not before we introduced some damping to the model. The damping coefficients were based on a free vibration study of the loaded shell prior to the collapse point.

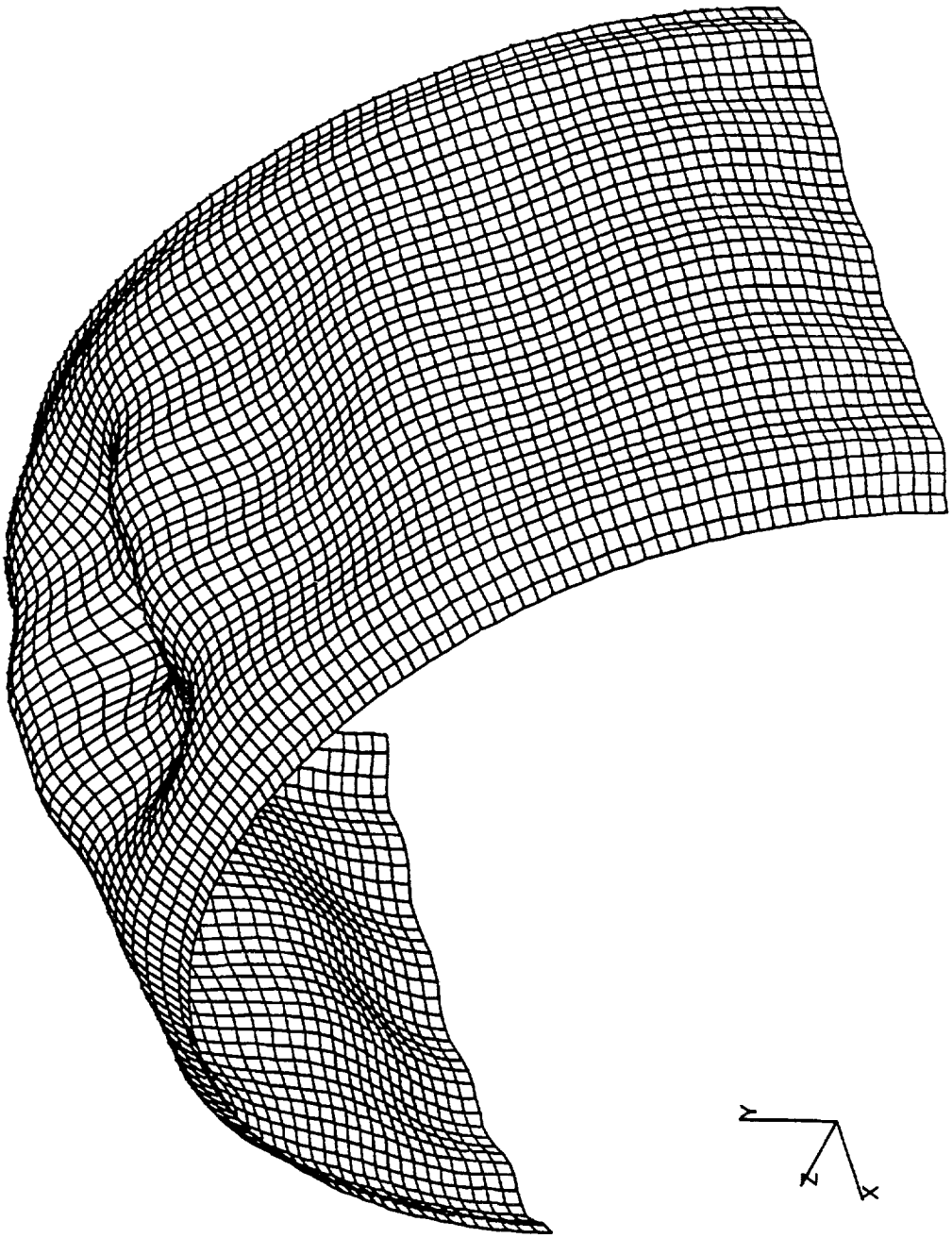

Figure 3 The pre-buckling state

(not to scale)

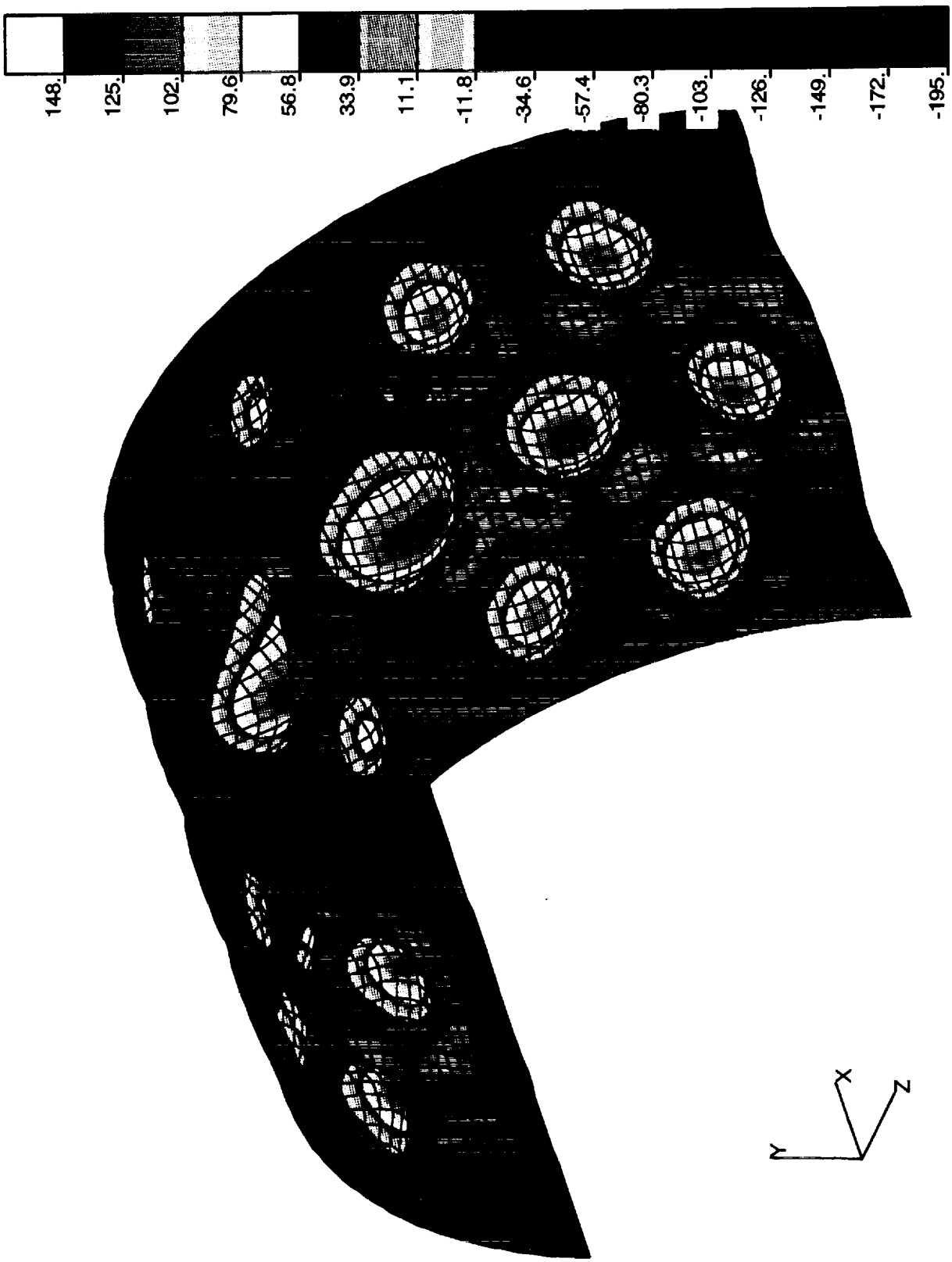

Figure 4 State of deformation at the beginning of the snapping motion

(not to scale)

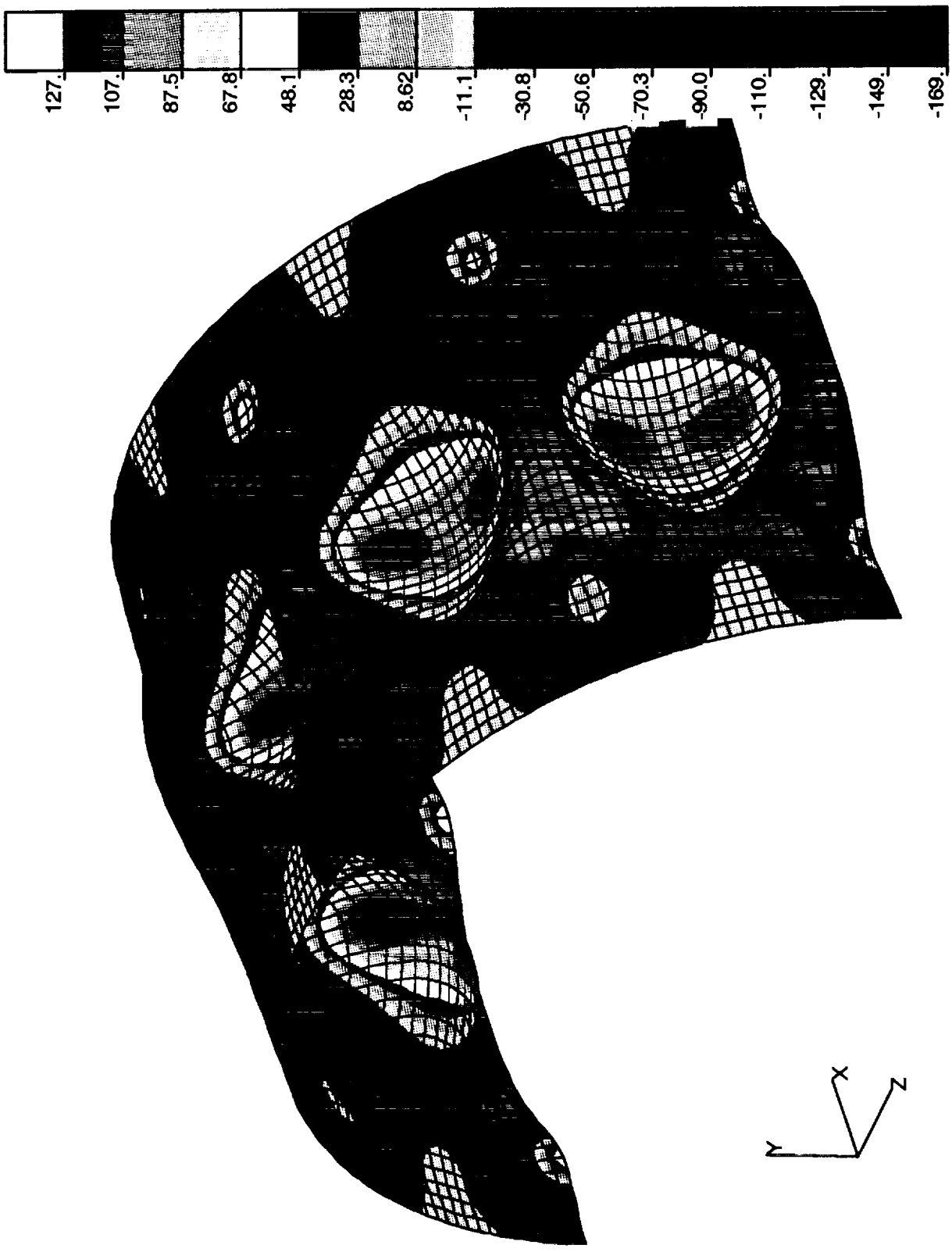

Figure 5 Stable postbuckling state

(not to scale)

For the initial conditions we chose: Starting configuration $\mathbf{d}(0) = \mathbf{d}_k$ [2]. End-shortening $\Delta u = \Delta u_k + e > \Delta u^*$; where Δu^* is the value that corresponds to the limit point ($\mathbf{d}^*$; Δu^*) and e is a small positive number. Initial velocity $\mathbf{d}' = \mathbf{0}$. The end-shortening Δu was kept constant during the dynamic response calculations. Note that the starting configuration chosen in this way *cannot* be close to an equilibrium state because the end-shortening is above the limiting value Δu^*.

For the dynamic response calculation we used the implicit method available in STAGS which was developed by Parks (Ref. 5, 11). The number of time steps that were needed to reach a new stable equilibrium state was 211. During the buckling process the kinetic energy increases from zero to a number of peak values before it goes to zero again when the structure comes to rest. According to our calculations, the time interval between the beginning of the snapping process and the moment at which the cylinder comes to full rest is of the order of magnitude of $O(10^{-1}$ sec). The stability of this new state was checked by switching the time integration procedure to the quasi static solution procedure. (Note that the stability of an equilibrium state is marked by a positive definite tangent stiffness matrix). It is of interest to note that the buckling mode pattern during the dynamic snap changed from 14 full waves in circumferential direction at the start of the snapping process [3] (Figure 4) to 10 full waves in the stable post -snapping state (Figure 5). The 14 full waves that are present near the limit point are due to the simplified (symmetrical) imperfection pattern that was used for this model. On the other hand, the 10 full waves (at displacements of the order of magnitude of 30 times wall the thickness (crest to crest of the waves)) in the post-snapping state correspond to what was observed in the experiment (Ref. 2).

It is finally noted that the results presented here were obtained on a Sun 4 work station after many nightly hours of operation.

5. Conclusion

We have shown in this paper that the numerical simulation of an actual buckling process is feasible with a present day finite element code. Although the model considered here is still one step away from the full scale experimental model with its measured imperfections (Ref. 2, 4), it contained nevertheless all the ingredients that are necessary for a full scale analysis. It seems to us that the approach sketched here could be of use for problems of a more practical nature. In particular, we believe that the method will be useful for the solution of so-called mode jumping problems that occur with axially compressed stiffened panels.

---

[2] Step 13 of the first static run.

[3] This is the 53^{th} step of the time integration procedure. Note that the displacement patterns displayed in Figure 3,4 and 5 are not at the same scale. The displacements in Figure 5 are roughly 10 times larger than in Figure 4.

References

1. Esslinger M., "Hochgeschwindigkeitaufnahmen von Beulvorgäng Dünnwandiger, Axial Belasteter Zylinder", Der Stahlbau, 31, (1970) 73- 76.

2. Singer J., Arbocz J. and Babcock Jr. C. D. "Buckling of Imperfect Stiffened Cylindrical Shells under axial Compression" AIAA Journal, Vol. 9, No. 1, Jan 1971, pp 68 - 75.

3. Thompson J.M.T., Hunt G.W., "A General Theory of Elastic Stability," John Wiley & Sons, Ltd., (1973).

4. Arbocz J. and Babcock Jr. C. D.," Utilization of STAGS to Determine the Knockdown Factors from Measured Initial Imperfections, Report LR - 275, Dept. of Aerospace Engng., Technical University of Delft, Delft, The Netherlands, 1978.

5. Almroth B.O., Brogan F.A., "Structural Analysis of General Shells, Volume II, User's Instructions for STAGSC-1", LMSC-D633873, Lockheed Palo Alto Research Lab., Palo Alto, CA. Dec. (1982)

6. Rankin C. C. and Brogan F. A. (1991), "The Computational Structural Mechanics Testbed Structural Element Processor ES5: STAGS Shell Element", Lockheed missiles & Space CO., Palo Alto, California, NASA Contractor Report 4358.

7. Rankin C. C. and Brogan F. A., "An Element Independent Corotational Procedure for the Treatment of Large Rotations," J. Pressure Vessel Techn., **108**, pp. 165 - 174, (1986).

8. Rankin C. C. and Nour-Omid B.,"The Use of Projectors to Improve Finite Element Performance," Computers & Structures, Vol. 30, No. 1/2, November, 1988, pp. 257-267.

9. Riks E., "Some Computational Aspects of The Stability Analysis of Nonlinear Structures", Comp. Meth. in Appl. Mech. and Engng. **47**. 219-259, 1984.

10. Riks E., "Progress in Collapse Analysis", Journal of Pressure Vessel Technology, Vol. 109/**27** - **41**,. Febr.1987.

11. Parks K. C., "Evaluating Time Integration Methods for Nonlinear Dynamic Analysis", in: Finite Element Analysis for Transient Nonlinear Behavior, T. Belytschko, J. R. Osias and P. V. Marcal eds., Applied Mechanics Symposia Series (AMSE New York 1975).